

Primary photochemical processes for PtCl_6^{2-} complex in acetonitrile solutions



Svetlana G. Matveeva^a, Ivan P. Pozdnyakov^{a,b}, Vjacheslav P. Grivin^a, Victor F. Plyusnin^{a,b},
Andrey S. Mereshchenko^c, Alexey A. Melnikov^d, Sergey V. Chekalin^d,
Evgeni M. Glebov^{a,b,*}

^a Voevodsky Institute of Chemical Kinetics and Combustion, Siberian Branch of the Russian Academy of Sciences, 3 Institutskaya Str., 630090 Novosibirsk, Russian Federation

^b Novosibirsk State University, 2 Pirogova Str., 630090 Novosibirsk, Russian Federation

^c Institute of Chemistry, Saint Petersburg State University, 26 Universitetskii pr., 198504 Saint-Petersburg, Russian Federation

^d Institute of Spectroscopy, Russian Academy of Sciences, 5 Fizicheskaya Str., 142190 Troitsk, Moscow, Russian Federation

ARTICLE INFO

Article history:

Received 19 January 2016

Received in revised form 26 March 2016

Accepted 27 March 2016

Available online 6 April 2016

Keywords:

Photosolvation

Chain photochemical processes

Primary photochemical process

Electron transfer

Hexachloroplatinate(IV)

Laser flash photolysis

Ultrafast kinetic spectroscopy

ABSTRACT

Photosolvation of hexachloroplatinate(IV) in acetonitrile with the formation of the $\text{Pt}^{\text{IV}}\text{Cl}_5(\text{CH}_3\text{CN})^-$ complex was studied in the time range from hundreds of femtoseconds to seconds. The primary Pt(III) intermediate was recorded and interpreted as the primary Adamson radical pair $[\text{Pt}^{\text{III}}\text{Cl}_5^{2-}(\text{C}_4\text{N}) \cdot \cdot \text{Cl}^{\bullet}]$, which then accepts an electron from a solvent molecule. Two successive Pt(III) intermediates recorded in time range from microseconds to tens of milliseconds were interpreted as $\text{Pt}^{\text{III}}\text{Cl}_5^{2-}(\text{C}_4\text{N})$ and $\text{Pt}^{\text{III}}\text{Cl}_4^-$ complexes. $\text{Pt}^{\text{III}}\text{Cl}_4^-$ was proposed to be a chain carrier in the chain photosolvation process. Dependencies of quantum yield of photosolvation on the initial complex concentration and excited light intensity were fitted in the framework of the proposed chain mechanism. Rate constants of the reactions of intermediates were determined.

© 2016 Elsevier B.V. All rights reserved.

1. Introduction

A fundamental problem in photocatalysis is to expand the absorption spectra of semiconductors (TiO_2 , CdS) into the visible spectral region. One of the useful methods to solve this problem is the modification of TiO_2 [1–5] and CdS [6–8] surfaces by metallic platinum via photoreduction of hexachloroplatinate. The process of four-electron photoreduction of Pt^{IV} to Pt^{0} in water-alcohol mixtures discovered by Cameron and Bocarsly [9,10] marked the beginning of using PtCl_6^{2-} photolysis as a tool for the fabrication of platinum nanoparticles [11–18]. For complete description of photochemical processes in the mentioned systems, the mechanisms of both heterogeneous and homogeneous processes should be taken into account. This is the main factor defining our motivation in studying $\text{Pt}^{\text{IV}}\text{Cl}_6^{2-}$ photochemistry.

The photochemistry of this complex is solvent-dependent (see [19] and references there). In aqueous solutions, the integral photochemical process is photoaquation with the formation of the $\text{Pt}^{\text{IV}}\text{Cl}_5(\text{H}_2\text{O})^-$ complex as primary photoproduct [20–27]. Mechanism of photoaquation includes redox stages. Starting with [28], in the most of papers on the photochemistry of aqueous $\text{Pt}^{\text{IV}}\text{Cl}_6^{2-}$ solutions, a homolytic cleavage of Pt–Cl bond with a chlorine atom escape into the solution bulk (1) was considered as the primary photochemical process.



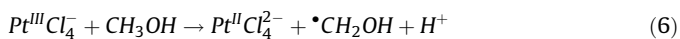
Intermediates interpreted as Pt(III) species were recorded in the experiments with microsecond [21,25], picosecond [29] and femtosecond [26,27,30] time resolution. When the primary process (1) is realized, photoaquation can follow a chain mechanism. Depending on the experimental parameters, quantum yield could be both less [20,21,25] and sufficiently higher than unity [20,22,27].

In alcoholic solutions of $\text{Pt}^{\text{IV}}\text{Cl}_6^{2-}$, the near UV excitation results in parallel processes of photosolvation and photoreduction [30]. Photoreduction is caused by an electron transfer from a solvent

* Corresponding author at: Voevodsky Institute of Chemical Kinetics and Combustion, Siberian Branch of the Russian Academy of Sciences, 3 Institutskaya Str., 630090 Novosibirsk, Russian Federation.

E-mail address: glebov@kinetics.nsc.ru (E.M. Glebov).

molecule to the light-excited complex [31–33] with the formation of Pt(III) intermediate – Pt^{III}Cl₆³⁻ complex, and a hydroxyalkyl radical. Pt^{III}Cl₆³⁻ complex rapidly dissociates to Pt^{III}Cl₅²⁻ and Cl⁻ [33]. In turn, Pt^{III}Cl₅²⁻ intermediate gives rise to the relatively long-living Pt^{III}Cl₄⁻ complex. The reaction scheme (for the case of methanol solutions) is described by Reactions (2)–(6).



This mechanism was supported by the experiments on ultrafast pump-probe spectroscopy [25,27]. The photochemical kinetics of Pt^{IV}Cl₆²⁻ reduction to Pt⁰ in methanol was recently studied by Wojnicki and Kwolek [34].

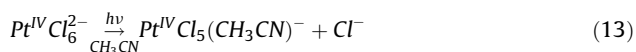
As for other organic solvents, photoreduction via the primary process (1) was reported to occur in the case of Pt^{IV}Cl₆²⁻ irradiation in chloroform solutions [35,36]. The following scheme including the reaction of $\bullet CCl_3$ radical with the initial complex was proposed (in assumption that the relevant species are protonated):



The mechanism (Eqs. (7)–(12)) was put forward based on the results of steady-state photolysis experiments and was supported by the proportionality of the initial rate of photolysis to the square root of intensity, which could be derived from the mechanism (Eqs. (7)–(12)) in the case of quasy-stationary conditions.

In the only work on the photolysis of Pt^{IV}Cl₆²⁻ in acetonitrile solutions [37] the following conclusions were made:

- (i) The integral photochemical reaction is photosolvation (13). This conclusion was made based on the quantitative release of free Cl⁻ anions and on the conservation of the isosbestic points in the course of photolysis.



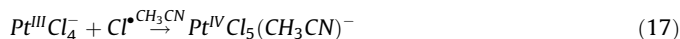
- (ii) The quantum yield is not wavelength-dependent in the region of 254–436 nm
- (iii) The quantum yield linearly depends on the concentration of the initial complex and on the reciprocal square root of light intensity, being higher than unity. The reported values of

quantum yield lie in the interval 1.2–5.5, i.e. chain processes are involved.

- (iv) In the lamp flash photolysis experiments (irradiation was performed by 50 μs pulses) an intermediate absorption with the maximum in the region of 530 nm was observed and attributed to Pt(III) intermediate. This intermediate was proposed to be Pt^{III}Cl₅²⁻ complex with the geometry of a square pyramid. The attribution was based on the calculations of Pt(III) intermediates optical spectra performed in [38].

Based on the points (i–iv), the authors [37] proposed the following mechanism (further called Mechanism A) of the processes starting from the primary process (1)

Mechanism A



In this work, nanosecond laser flash photolysis was applied to examine the mechanism of photolysis (Eqs. (14)–(17)). The general idea was to quantify the amount of chlorine atoms formed in the primary process (1) by means of their scavenging with free Cl⁻ ions and registration of Cl₂^{•-} radical anions which demonstrate a well-known characteristic spectrum in the near UV spectral range [39]. In addition, the primary photophysical processes were studied by means of ultrafast kinetic spectroscopy.

2. Experimental

Solutions of Pt^{IV}Cl₆²⁻ complex were prepared from Na₂PtCl₆ salt (Aldrich). Chemically pure grade LiCl and NEt₄Cl were used as sources of free Cl⁻ anions. Solutions for photochemical experiments were prepared using spectrophotometrically grade acetonitrile (Cryochrom, Russia).

UV absorption spectra were recorded using Agilent 8453 (Agilent Technologies) and Varian Cary 50 (Varian Inc.) spectrophotometers. Stationary photolysis was performed using the irradiation of a XeBr (282 nm) barrier discharge exciplex lamp (excilamp) [40] produced by the Institute of High Current Electronics, Siberian Branch of the Russian Academy of Sciences, Tomsk, Russia. The parameters of irradiation were: bandwidth Δl ca. 5 nm, peak output power W_{peak} = 19 mW/cm², frequency f = 200 kHz, and pulse duration ca. 1 μs. The incident light intensity was typically ca. 2.7 × 10¹⁶ photons s⁻¹ cm⁻². Quantitative measurements of quantum yields of Pt^{IV}Cl₆²⁻ photosolvation in the course of laser photolysis were performed using the irradiation of an LS-2137U Nd:YAG laser (Lotis TII, Belarus) with excitation wavelengths of 266 nm and pulse duration of ca. 5 ns.

The laser flash photolysis setup was based on the up-mentioned Nd:YAG laser. The illumination spot area was ca. 0.1 cm² and energy per pulse was up to 20 mJ; the setup was similar to that described in Ref. [41]. The overall time resolution of the setup was 50 ns. For the time interval 50–800 μs probing was performed by a xenon lamp operated in the pulsed mode for increasing the light intensity. In the case of experiments performed in the long time interval (1–50 ms) the probing was performed by means of irradiation of light-emitted diodes HPL-H77 (High Power Lighting

Corp., Taiwan). For the extraction of reaction rate constants from the experimental data, a system of differential equations corresponding to the selected reaction scheme was solved numerically by a fourth-order Runge-Kutta method, and the results were compared with the experimental kinetic curves.

Pump-probe spectroscopy was used to study transient absorption of the samples in picosecond time domains. The experimental setup was described in detail in Ref. [42]. The samples were excited by ~60 fs pulses (energy ca. 1 μ J, pulse repetition rate 1 kHz) at ~400 nm (second harmonic of a Ti:sapphire generator-amplifier system, CDP Ltd., Moscow, Russia). 200 pulses were used to record a single time-resolved spectrum. Each kinetic curve contains 110 points (60 points with a 100 fs step, 20 points with a 500 fs step, and 30 points with a 3 ps step). The investigated solutions (total volume of 20 ml) were pumped through a 1 mm cell at room temperature to provide uniform irradiation and avoid possible degradation due to photochemical reactions. The experimental data were globally fitted by a three-exponential model. The fitting program performed corrections of the group velocity dispersion and calculated the response time of the instrument.

3. Results and discussions

3.1. UV spectra and photochemistry of $\text{Pt}^{\text{IV}}\text{Cl}_6^{2-}$ complex in CH_3CN

Platinum(IV), which has the d^6 electronic configuration, forms stable and kinetically inert complexes with a variety of ligands. $\text{Pt}^{\text{IV}}\text{Cl}_6^{2-}$ is a low-spin complex with octahedral symmetry. The intense ($\epsilon = 23700 \text{ M}^{-1} \text{ cm}^{-1}$, which corresponds well with the value $23600 \text{ M}^{-1} \text{ cm}^{-1}$ reported for an aqueous solution [20]) charge transfer band with maximum at 270 nm (curve 1 in Fig. 1) corresponds to the transitions from π -orbitals of ligands to a metal center [43,44]. It should be noted that this band in CH_3CN demonstrates an 8 nm red shift in comparison with the case of aqueous solution [43]. A shoulder in the region of 355 nm and a low intensity broad band with maximum at 455 nm belong to d-d transitions [43,44].

Changes in the UV spectrum caused by the stationary photolysis (286 nm) of $\text{Pt}^{\text{IV}}\text{Cl}_6^{2-}$ solution in acetonitrile are shown in Fig. 1. The conservation of two isosbestic points (249 and 313 nm) indicates the appearance of only one photolysis product. Quantitative release of Cl^- anions in the course of photolysis reported in [37] indicates that photosolvation (13) is the only observed photochemical process. The changes in the UV absorption spectra in the

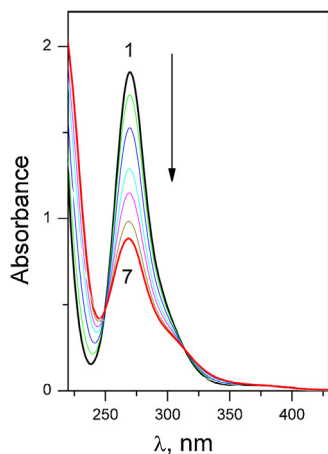


Fig. 1. Changes in the UV absorption spectrum caused by irradiation (286 nm) of $\text{Pt}^{\text{IV}}\text{Cl}_6^{2-}$ in acetonitrile solution (1 cm cell, initial concentration $7.8 \times 10^{-5} \text{ M}$). Curves 1–7 correspond to 0; 2; 5; 7; 10; 21; 47 s of irradiation.

case of laser photolysis of $\text{Pt}^{\text{IV}}\text{Cl}_6^{2-}$ at 266 nm were the same as in the case of the excilamp irradiation, therefore, the reaction pathway does not depend on the exciting light intensity. No effect of the dissolved oxygen on the rate of photolysis was observed.

3.2. Formation and decay of Pt(III) intermediates

The experiments on the laser flash photolysis of $\text{Pt}^{\text{IV}}\text{Cl}_6^{2-}$ in acetonitrile have demonstrated the formation of intermediate absorption, which kinetic behaviour is rather complicated. The typical kinetic curves in time range from tens of microseconds to tens of milliseconds are shown in Fig. 2. For clarity, kinetic curves at three time domains are presented (Fig. 2a–c). The characteristic time of the intermediate absorption formation was less than the time resolution of the experimental setup (50 ns). The kinetic curves were fitted using a kinetic scheme discussed below (fit curves are represented by black lines in Fig. 2).

The evolution of the intermediate absorption spectrum is shown in Fig. 3. Two intermediate absorption bands with the maxima in the regions of 540 and 410 (curve 1 in Fig. 3) nm were attributed to the $\text{Pt}^{\text{III}}\text{Cl}_5^{2-}$ complex with the structure of a square pyramid (C_{4v}) and sufficient elongation of the bond $\text{Pt} - \text{Cl}_{\text{ax}}$. This assignment is based on the relativistic $X\alpha$ calculations of possible Pt(III) intermediates performed by Goursot et al. in the 80th years of XX century [38]. Previously this intermediate was recorded in the course of $\text{Pt}^{\text{IV}}\text{Cl}_6^{2-}$ photolysis in alcohol solutions [31–33], but not in aqueous solutions [25].

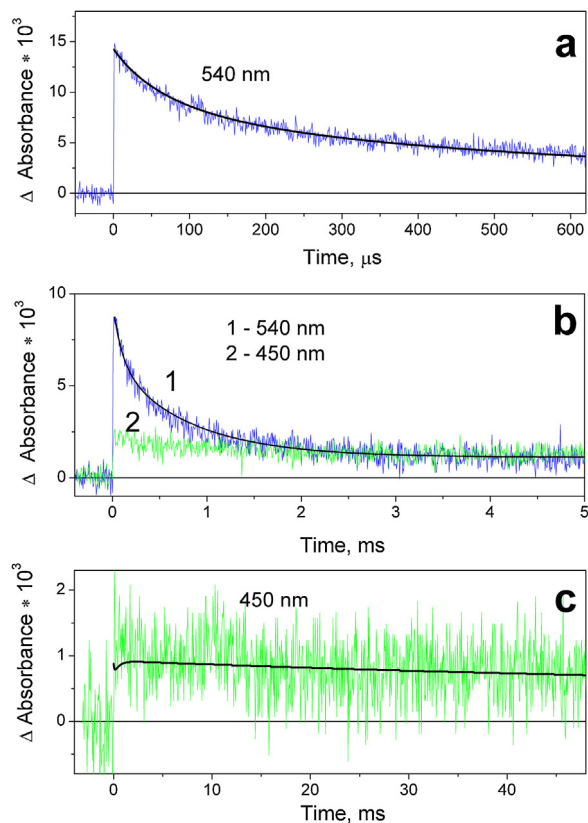


Fig. 2. Laser flash photolysis (266 nm, 6 mJ/pulse) of PtCl_6^{2-} in CH_3CN (1 cm cell, initial concentration $2.7 \times 10^{-5} \text{ M}$, natural content of oxygen) at different time domains. Experimental curves (noisy lines) and their fits (smooth lines) using Mechanism B (see Section 3.4. for details) with parameters $\epsilon_{540 \text{ nm}}(\text{Pt}^{\text{III}}\text{Cl}_5^{2-}) = 1200 \text{ M}^{-1} \text{ s}^{-1}$, $\epsilon_{450 \text{ nm}}(\text{Pt}^{\text{III}}\text{Cl}_4^-) = 200 \text{ M}^{-1} \text{ s}^{-1}$, $k_{16} = 1.2 \times 10^5 \text{ M}^{-1} \text{ s}^{-1}$, $k_{24} = 1 \times 10^6 \text{ M}^{-1} \text{ s}^{-1}$, $k_{25} = 6 \times 10^8 \text{ M}^{-1} \text{ s}^{-1}$, $k_{26} = 5 \times 10^3 \text{ M}^{-1} \text{ s}^{-1}$. (a) Time scale 600 μ s; $k_{15} = 1500 \text{ s}^{-1}$; (b) time scale 5 ms, $k_{15} = 1500 \text{ s}^{-1}$; (c) time scale 50 ms, $k_{15} = 1200 \text{ s}^{-1}$.

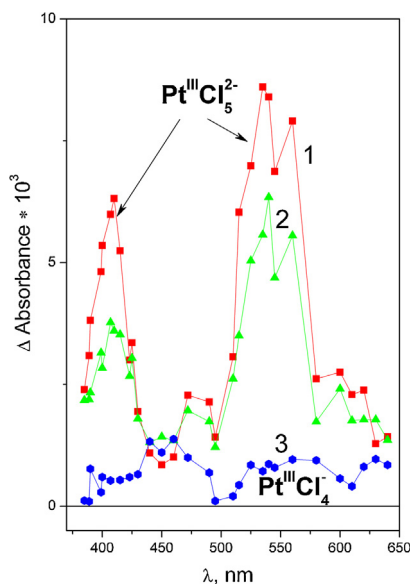


Fig. 3. Laser flash photolysis (266 nm, ca. 6 mJ/pulse) of PtCl_6^{2-} in CH_3CN (1 cm cell, initial concentration 2.7×10^{-5} M), 6 ms time scale. Intermediate absorption spectra. Curves 1–3 correspond to 0; 0.13 and 6 ms after laser pulse.

After decaying of absorption attributed to $\text{Pt}^{\text{III}}\text{Cl}_5^{2-}$, a noticeable residual absorption remains in the region of 450 and 620 nm. Its spectrum is represented by curve 3 in Fig. 3. In turn, this absorption does not remain constant and slowly decays with the characteristic time of ca. 0.1 s (Fig. 2c). In spite of a rather low signal, the tendency of the decay clearly manifests itself. This slowly decaying absorption was attributed to the second intermediate of Pt(III), namely, to the flat complex $\text{Pt}^{\text{III}}\text{Cl}_4^-$. The interpretation, as in the case of the first intermediate, was based on the calculations performed by Goursot et al. [45]. As it would be shown later, the second Pt(III) intermediate plays the role of the chain carrier in the process of the chain photosolvation of $\text{Pt}^{\text{IV}}\text{Cl}_6^{2-}$ (Eq. (16)).

To estimate the molar absorption coefficients and quantum yields of intermediates formation, the initial absorption of $\text{Pt}^{\text{III}}\text{Cl}_5^{2-}$ was plotted as a function of the incident laser pulse energy (Fig. 4a). The corresponding dependence is linear at low energies with a trend to saturation at higher energies. This type of dependence is typical for a one-photon process. Following the work [46], we have fitted the experimental curve by function (18):

$$\Delta A = a(1 - e^{-bh}) \quad (18)$$

where ΔA is the intermediate absorption at the registration wavelength and h (in work [46] it was measured in photons/cm²) is the light flux per unit area.

In principle, saturation of the dependence (Fig. 4a) could be explained by two factors. First, one could assume that the intermediate photolysis product absorbs at the wavelength of excitation (266 nm), and the characteristic time of its formation is small in comparison with the laser pulse duration (5 ns). In this case, the new product should compete for the light quanta with the initial $\text{Pt}^{\text{IV}}\text{Cl}_6^{2-}$ complex, which should result in saturation of the dependence of intermediate absorption vs. laser pulse energy. Nevertheless, in our case the intermediate does not absorb significantly in the region of wavelengths shorter than 370 nm, and the corresponding explanation of saturation could be ruled out.

Another (and simpler) explanation of saturation is the limited amount of initial substance in comparison with the amount of the incident light quanta. If all the irradiated $\text{Pt}^{\text{IV}}\text{Cl}_6^{2-}$ complexes are

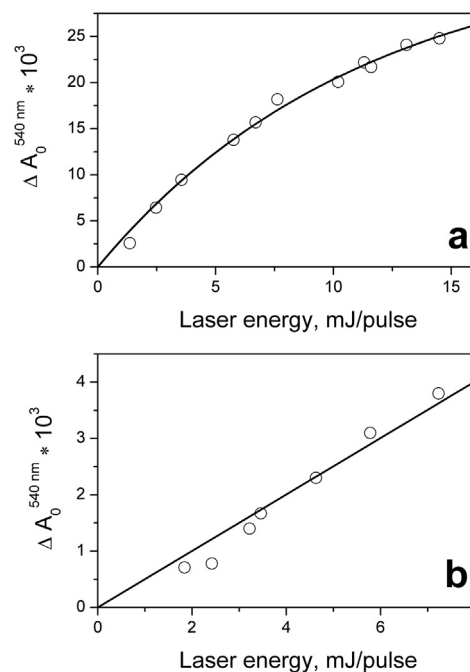


Fig. 4. Dependence of initial $\text{Pt}^{\text{III}}\text{Cl}_5^{2-}$ absorption (540 nm) in the course of laser flash photolysis (266 nm) of PtCl_6^{2-} in CH_3CN vs. energy of laser pulses. 1 cm cell, diameter of irradiated spot of the sample 2 mm (a) initial concentration 2.7×10^{-5} M (absorption at 266 nm is 0.61). Experimental points and best fit by Eq. (18). (b) initial concentration 4.4×10^{-6} M (absorption at 266 nm is 0.1). Experimental points and linear fit.

converted to products, the further increase in light quanta flux would not result in the intermediate absorption increase. Therefore, fitting parameter a in Eq. (18) allows one to estimate molar absorption coefficient of intermediate ε_{int}

$$a = \varepsilon_{\text{int}} c_0 l \quad (19)$$

where c_0 is the concentration of the initial compound ($\text{Pt}^{\text{IV}}\text{Cl}_6^{2-}$ in our case), l is the optical path length.

The validity of Eq. (19) does not depend on the concentration of the initial compound. In addition, as it was shown in Ref. [46], if the absorption of the initial reagent at the excitation wavelengths A_{ex} is small, one can use the parameter b in Eq. (18) to calculate the quantum yield of the formation of intermediate (ϕ)

$$b = \phi \sigma_{\text{ex}} \quad (20)$$

where σ_{ex} is the absorption cross section (in cm³) of the initial compound at the excitation wavelengths, which is related to the molar absorption coefficient as $\sigma_{\text{ex}} = 3.82 \times 10^{-21} \varepsilon_{\text{ex}}$ (ε_{ex} is the molar absorption coefficient of the initial compound at the excitation wavelength measured in M⁻¹ cm⁻¹). In the experiment shown in Fig. 4a the value of A_{ex} was not chosen small in order to observe the trend to saturation, therefore, the calculation of quantum yield using Eq. (20) was not perfect enough. To estimate the quantum yield, the experiments with the small concentration of the initial complex were performed (Fig. 4b). In this case, saturation could not be achieved, but the tangent of linear dependence of intermediate absorption vs. laser pulse energy allows one to calculate the quantum yield. Combining Eq. (18) at $bh \ll 1$ with Eqs. (19) and (20), we obtain

$$\Delta A = a \sigma_{\text{ex}} \phi h \quad (21)$$

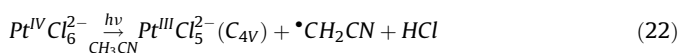
Using Eq. (18) to fit the dependence in Fig. 4a and Eq. (21) to fit the dependence in Fig. 4b, we have calculated the values of molar

absorption coefficient of $\text{Pt}^{\text{III}}\text{Cl}_5^{2-}$ at 540 nm and quantum yield of its formation upon 266 nm excitation. The corresponding values are $\varepsilon_{\text{int}}^{540\text{nm}} = 1200 \pm 200 \text{ M}^{-1}\cdot\text{cm}^{-1}$ and $\phi^{266\text{nm}} = 0.028 \pm 0.04$. It should be noted that the molar absorption coefficient of $\text{Pt}^{\text{III}}\text{Cl}_5^{2-}$ in methanol solutions reported in Ref. [31] was $3000 \pm 600 \text{ M}^{-1}\text{cm}^{-1}$ at 535 nm. Therefore, the molar absorption coefficient of this intermediate is solvent-dependent, which is indicative of the strong interaction between Pt(III) cation and a solvent molecule.

Using Fig. 3, one can estimate the molar absorption coefficient of the $\text{Pt}^{\text{III}}\text{Cl}_4^-$ intermediate in the region of 440–460 nm as $200 \pm 50 \text{ M}^{-1}\text{cm}^{-1}$.

3.3. Primary photochemical process: inner-sphere or inter-sphere electron transfer?

Formation of the primary Pt(III) intermediate could be assumed as the result of the inner-sphere electron transfer mechanism A. Another possibility is the inter-sphere electron transfer from the solvent molecule to the light-excited complex, like in the case of alcoholic solutions (Reactions (2)–(6)). For acetonitrile solutions, the total equation of the primary photochemical process could be written as



In order to choose one of the primary processes (14) and (22) the experiments on the laser flash photolysis of $\text{Pt}^{\text{IV}}\text{Cl}_6^{2-}$ in the presence of free Cl^- anions were performed. The reaction between a chlorine atom and Cl^- (23) is diffusion-controlled [47].



Estimating its rate constant as $10^{10} \text{ M}^{-1}\text{s}^{-1}$, we obtain that when the concentration of free Cl^- anions is about 10^{-3} M , the characteristic time of $\text{Cl}_2^{\bullet-}$ formation is about 100 ns. Considering Reaction (14) as the primary photochemical process, one could expect that in the experiments performed with our laser flash photolysis setup the formation of the $\text{Cl}_2^{\bullet-}$ radical anions absorption should occur immediately after the laser pulse. This radical anion exhibits a strong absorption band with the maximum at 350 nm and molar absorption coefficient $9600 \text{ M}^{-1}\text{cm}^{-1}$ (in aqueous solutions) [48].

When performing experiments in aprotic solvents like acetonitrile, the peculiarities of the solvation of ions should be taken into account. For example, the alkali halides in acetonitrile demonstrate rather high association constants [49]. As a result, even at millimolar concentrations of salts the molecular form could be predominant in solutions. Let us consider lithium chloride, which solubility in acetonitrile is 0.0257 g/L at 23 °C [50]. The association constant for the pair $\text{Li}^+ - \text{Cl}^-$ is 2915 M^{-1} [49]. The calculated concentration of free Cl^- ions in CH_3CN as a function of LiCl concentration is shown in Fig. 5 (Curve 1). One can see that at 0.01 M of loaded LiCl the concentration of free chloride ions is $1.7 \times 10^{-3} \text{ M}$. For the case of NEt_4Cl the association constant in acetonitrile is 14 M^{-1} [51]. This value is two orders of magnitude less than for LiCl. For 0.01 M of loaded NEt_4Cl the content of free Cl^- anions in solution is about 88% (Curve 2 in Fig. 5). In our experiments on $\text{Pt}^{\text{IV}}\text{Cl}_6^{2-}$ photolysis both LiCl and NEt_4Cl were used as the sources of free Cl^- anions.

If the primary photochemical process is Reaction (14), the photolysis of $\text{Pt}^{\text{IV}}\text{Cl}_6^{2-}$ in the presence of 0.01 M of both NEt_4Cl and LiCl should result in the full conversion of chlorine atoms to $\text{Cl}_2^{\bullet-}$. According to the ratio of the maximal absorption coefficients of $\text{Cl}_2^{\bullet-}$ and $\text{Pt}^{\text{III}}\text{Cl}_5^{2-}$, the initial absorption of $\text{Cl}_2^{\bullet-}$ at 350 nm should be three times higher than the initial absorption of $\text{Pt}^{\text{III}}\text{Cl}_5^{2-}$ at 540 nm. However, no evidence of $\text{Cl}_2^{\bullet-}$ absorption was obtained in

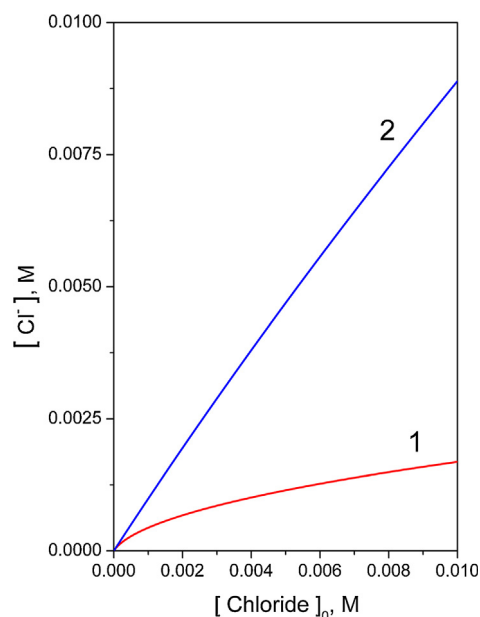


Fig. 5. Concentration of free Cl^- anions in solutions of LiCl (1) and NEt_4Cl (2) in acetonitrile as a function of the salt concentration. Calculation using the association constants 2915 [50] and 14 M^{-1} [51] for LiCl and NEt_4Cl correspondingly.

our experiments. Therefore, the mechanism of photolysis starting from the chlorine atom escape to the solution bulk (14) could be ruled out.

The only possible mechanism explaining Pt(III) formation is the inter-sphere electron transfer via Reaction (22), as in the case of alcoholic solutions described in Introduction. It should be noted that both cyanomethyl radical $\cdot\text{CH}_2\text{CN}$ formed in this reaction and the corresponding peroxy radical $\cdot\text{OOCH}_2\text{CN}$ absorb light in the wavelengths range 220–300 nm [52,53]. The maxima of the spectra of both radicals lie in the region of 230 nm, and molar absorption coefficients in the maxima were estimated as 1000 and $2200 \text{ M}^{-1}\text{cm}^{-1}$ for $\cdot\text{CH}_2\text{CN}$ and $\cdot\text{OOCH}_2\text{CN}$ correspondingly [53]. These radicals could not be detected in the course of our laser flash photolysis experiments because their absorption is shielded by different platinum species. Another possibility is performing experiments on stationary photolysis in frozen matrices at 77 K with the ESR detection of radicals, but it is not prospective because acetonitrile has no glass transition. Therefore, our evidence of the primary process (22) is indirect, but the proposed reaction mechanism is supported by all the data set presented in this work.

It should be noted that direct evidence of the proposed reaction mechanism could probably be obtained from the time-resolved ESR (TR ESR) detection of the $\cdot\text{CH}_2\text{CN}$ radical (it was observed using TR ESR upon photolysis of dibenzoyl peroxide in acetonitrile [54]).

3.4. Chain photosolvation of PtCl_6^{2-} in CH_3CN

After the formation of initial Pt(III) intermediate in Reaction (22), the chain photosolvation similar to that presented by Reactions ((15)–(17)) is expected. To examine the mechanism of photosolvation, we have measured the quantum yields of $\text{Pt}^{\text{IV}}\text{Cl}_6^{2-}$ disappearance at the same conditions as for the laser flash photolysis experiments. Quantum yields were calculated assuming that the $\text{Pt}^{\text{IV}}\text{Cl}_5(\text{CH}_3\text{CN})^-$ complex is the only reaction product. Its molar absorption coefficient at the wavelength at 270 nm (i.e. in the maximum of PtCl_6^{2-} absorption) was taken equal to that of $\text{Pt}^{\text{IV}}\text{Cl}_5(\text{H}_2\text{O})^-$ complex ($12500 \text{ M}^{-1}\text{cm}^{-1}$ [20]).

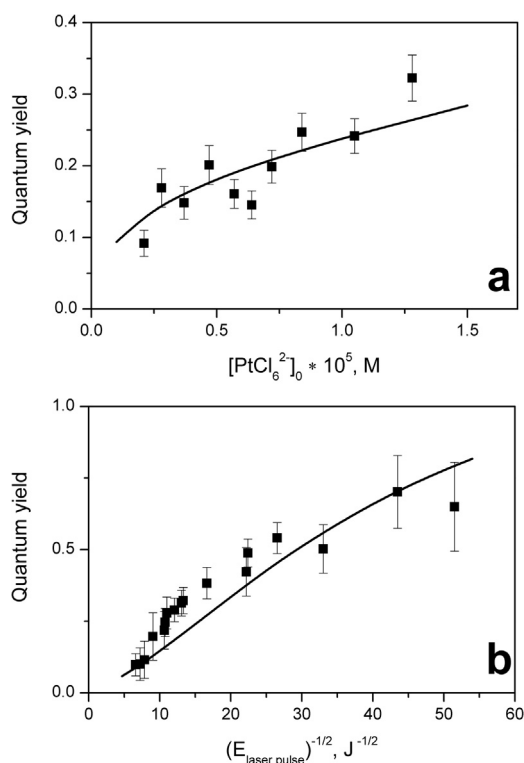


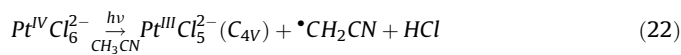
Fig. 6. Dependencies of quantum yield of $\text{Pt}^{\text{IV}}\text{Cl}_6^{2-}$ photosolvation (caused by laser photolysis at 266 nm, frequency of pulses 1 Hz) in CH_3CN vs. (a) initial concentration of $\text{Pt}^{\text{IV}}\text{Cl}_6^{2-}$ (laser energy 8 mJ/pulse) and (b) reciprocal square root from the laser pulse energy (initial concentration of $\text{Pt}^{\text{IV}}\text{Cl}_6^{2-}$ 10^{-5} M). 1 cm cell, air saturated solutions. Points – experimental data, solid curves – a fit of quantum yields in the framework of Mechanism B with the rate constants $k_{15}=1300\text{ s}^{-1}$, $k_{16}=1.2 \times 10^5\text{ M}^{-1}\text{ s}^{-1}$, $k_{24}=1 \times 10^6\text{ M}^{-1}\text{ s}^{-1}$, $k_{25}=6 \times 10^8\text{ M}^{-1}\text{ s}^{-1}$, $k_{26}=5 \times 10^3\text{ M}^{-1}\text{ s}^{-1}$. Quantum yield of $\text{Pt}^{\text{III}}\text{Cl}_5^{2-}$ formation was taken to 0.028.

The laser photolysis experiments were performed with excitation at 266 nm (laser pulse duration 5–6 ns and pulse frequency 1 Hz). The dependencies of the quantum yields of photosolvation vs. initial concentration $[\text{Pt}^{\text{IV}}\text{Cl}_6^{2-}]_0$ and reciprocal square root of the laser pulse energy ($E^{-1/2}$) are shown in Fig. 6. The dependencies of photosolvation quantum yield both on $[\text{Pt}^{\text{IV}}\text{Cl}_6^{2-}]_0$ (Fig. 6a) and on $E^{-1/2}$ (Fig. 6b); note that large experimental errors are essential for low laser pulse energies) are close to those obtained in the case of lamp stationary photolysis [37]. The dependencies in Fig. 6 testify in favour of chain mechanism of photosolvation. The increase of the quantum yield with the increase of $[\text{Pt}^{\text{IV}}\text{Cl}_6^{2-}]_0$ reflects the chain character of the process, while the dependence of quantum yield vs. $E^{-1/2}$ is caused by the second order decay of a chain carrier.

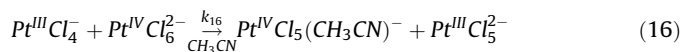
To compare the data on laser flash photolysis and stationary photolysis, the kinetic curves of intermediate absorption (Fig. 2) and dependencies of quantum yield on $[\text{Pt}^{\text{IV}}\text{Cl}_6^{2-}]_0$ and $E^{-1/2}$ (Fig. 6) were fitted using the same set of parameters. For complete description of chain reactions Mechanism A proposed in Ref. [37] was modified to Mechanism B (for convenience, we repeat here any of the reactions mentioned previously):

Mechanism B

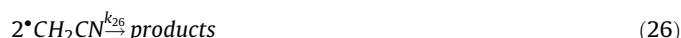
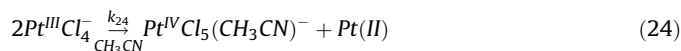
Chain initiation



Chain propagation



Chain decay



In this mechanism, the inter-sphere electron transfer (22) instead of the inner-sphere Reaction (14) is the primary photochemical process. The $\text{Pt}^{\text{III}}\text{Cl}_4^-$ complex is the chain carrier, as proposed in [37]. The chain decay occurs in Reactions (24) and (25) instead of Reaction (17) proposed in [37]. The introduction of the reactions of the cyanomethyl radical $\bullet\text{CH}_2\text{CN}$ (25) and (26) were necessary for the quantitative description of kinetic curves of the intermediate absorption.

All the kinetic curves obtained in the laser flash photolysis experiments were fitted in the framework of Mechanism B. The values of molar absorption coefficients for $\text{Pt}^{\text{III}}\text{Cl}_5^{2-}$ and $\text{Pt}^{\text{III}}\text{Cl}_4^-$ intermediates obtained from dependencies (Fig. 4) were used for fitting. The examples of kinetic curves and corresponding best fits are shown in Fig. 2. The rate constants corresponding to the best fits are collected in Table 1.

To ensure that the results of laser flash photolysis experiments and quantum yield dependencies on initial complex concentration and laser pulse energy (Fig. 6) are consistent, we performed modelling of corresponding dependencies using Mechanism B. The results are shown in Fig. 6 as solid lines. To mimic the dependence of quantum yield vs. initial concentration of the initial complex (Fig. 6a), we calculated the initial concentration of the first observed intermediate $[\text{Pt}^{\text{III}}\text{Cl}_5^{2-}]_0$ corresponding to the measured value of quantum yield ($\phi_0 = 0.028$) and experimental laser energy. Then the system of differential equations corresponding to Mechanism B was numerically solved to determine the final concentration of the solvated complex $[\text{Pt}^{\text{IV}}\text{Cl}_5(\text{CH}_3\text{CN})^-]_{\text{final}}$. The calculated quantum yield was determined as

$$\phi_{\text{calc}} = \phi_0 \frac{[\text{Pt}^{\text{III}}\text{Cl}_5(\text{CH}_3\text{CN})^-]_{\text{final}}}{[\text{Pt}^{\text{III}}\text{Cl}_5^{2-}]_0} \quad (27)$$

Using this approach, the best fit curve (solid line in Fig. 6a) was obtained using the set of rate constants listed in Table 1.

Table 1

Molar absorption coefficients of intermediates caused by laser flash photolysis of $\text{Pt}^{\text{IV}}\text{Cl}_6^{2-}$ in CH_3CN and rate constants of their reactions included to Mechanism B.

$\text{Pt}^{\text{III}}\text{Cl}_5^{2-}$ $\epsilon_{540\text{ nm}}$, $\text{M}^{-1}\text{ cm}^{-1}$	$\text{Pt}^{\text{III}}\text{Cl}_4^-$ $\epsilon_{450\text{ nm}}$, $\text{M}^{-1}\text{ cm}^{-1}$	k_{15} , s^{-1}	k_{16} , $\text{M}^{-1}\text{ s}^{-1}$	k_{24} , $\text{M}^{-1}\text{ s}^{-1}$	k_{25} , $\text{M}^{-1}\text{ s}^{-1}$	k_{26} , $\text{M}^{-1}\text{ s}^{-1}$
1200 ± 200	200 ± 50	$(1.3 \pm 0.3) \times 10^3$	$(1.2 \pm 0.2) \times 10^5$	$(1.0 \pm 0.2) \times 10^6$	$(6.0 \pm 1.0) \times 10^8$	$(5 \pm 1) \times 10^3$

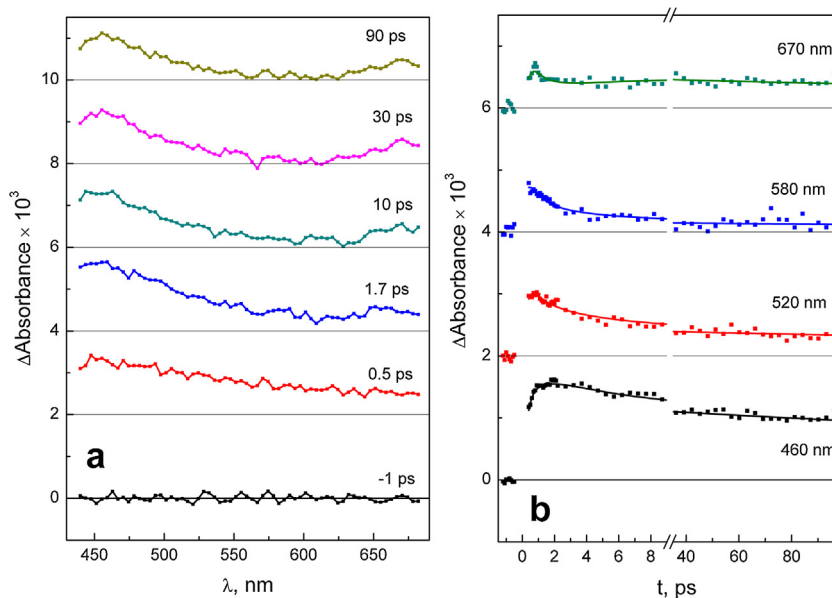


Fig. 7. Results of ultrafast kinetic spectroscopy experiments ($\lambda_{\text{pump}} = 400$ nm) with PtCl_6^{2-} (1.85×10^{-3} M) in CH_3CN solution. (a) Intermediate absorption spectra at different times, (b) experimental kinetic curves (dots) and three-exponential fits (solid lines).

The similar procedure was used to mimic the dependence of quantum yield vs. reciprocal square root of laser pulse energy (solid line in Fig. 6b). In this case, satisfactorily agreement between experimental and calculated dependencies was also achieved. Therefore, the description of different type experiments by the same set of kinetic parameters is an argument in favour of the proposed photolysis mechanism.

4. Ultrafast kinetic spectroscopy of $\text{Pt}^{\text{IV}}\text{Cl}_6^{2-}$ in CH_3CN

In the course of ultrafast kinetic spectroscopy experiments the intermediate absorption spectra were recorded in the range 440–680 nm (Fig. 7a). In the kinetic curves (Fig. 7b) the experimental points corresponding to time delays falling into the range (-500 fs) $< \tau >$ (300 fs) are omitted because they are affected to the coherent artifact caused by the coherent interactions between pump and probe pulses [55]. The kinetic curves obtained in the experiments on the ultrafast pump-probe spectroscopy were globally fitted using a triexponential function (28).

$$\Delta A(\lambda, t) = A_1(\lambda)e^{-k_1 t} + A_2(\lambda)e^{-k_2 t} + A_3(\lambda)e^{-k_3 t} \quad (28)$$

When the kinetic curves are fitted using the triexponential function (28), the sequential decay of the transient absorption $A \rightarrow B \rightarrow C \rightarrow$ (ground state + products) is proposed. The species associated difference spectra (SADS) of the individual components were calculated by means of the formulae derived in Ref. [56].

$$S_A(\lambda) = A_1(\lambda) + A_2(\lambda) + A_3(\lambda) \quad (29)$$

$$S_B(\lambda) = A_2(\lambda) \frac{k_1 - k_2}{k_1} + A_3(\lambda) \frac{k_1 - k_3}{k_1} \quad (30)$$

Table 2

The characteristic lifetimes of the primary processes followed by $\text{Pt}^{\text{IV}}\text{Cl}_6^{2-}$ irradiation (400 nm, 60 fs laser pulses) in CH_3CN .

Reaction	Characteristic lifetime, ps
33	0.8 ± 0.6
34	4.4 ± 1.9
35	370 ± 160

$$S_C(\lambda) = A_3(\lambda) \frac{(k_1 - k_3)(k_2 - k_3)}{k_1 k_2} \quad (31)$$

The global fit of experimental kinetic curves gave the characteristic times (which are the reciprocal constants k_i in Eq. (28)) collected in Table 2. The SADS of the intermediates are shown in Fig. 8. The spectra and kinetic behavior of the intermediate absorption bands formed by irradiation of $\text{Pt}^{\text{IV}}\text{Cl}_6^{2-}$ in CH_3CN are similar to the case of aqueous and alcoholic solutions [26,27,30]. Immediately after excitation the transient absorption spectrum appears as a wide band covering all the region of observation (440–680 nm, curve 1 in Fig. 8). The first process

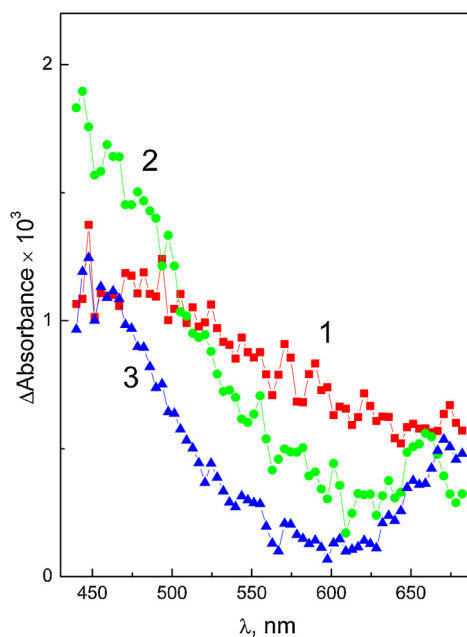
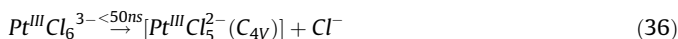
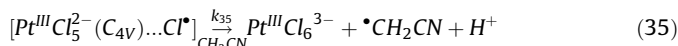
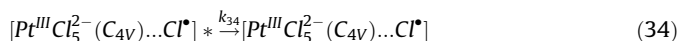
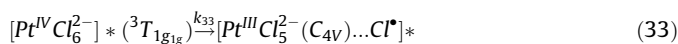


Fig. 8. Results of ultrafast kinetic spectroscopy experiments ($\lambda_{\text{pump}} = 400$ nm) with PtCl_6^{2-} (1.85×10^{-3} M) in CH_3CN solution. Species associated difference spectra (SADS) obtained from the three-exponential global fit (Eq. (24)) of kinetic curves (Fig. 7) and formulae (25–27).

results in formation of two absorption bands with the maxima at ≤ 450 nm and ≥ 660 nm (curve 2 in Fig. 8). The second process results in the narrowing of these bands without sufficient changes in their positions and relative intensities. The last process results in the uniform disappearance of intermediate absorption.

The similar behavior of the two bands at ≤ 450 and ≥ 660 nm means that they belong to the same intermediate. This intermediate was first observed by Goursot et al. [29] in the experiments on the 30 ps laser flash photolysis of aqueous PtCl_6^{2-} solutions. In Ref. [26], this intermediate was attributed (for both aqueous and alcoholic solutions) to the primary Adamson radical pair $[\text{Pt}^{\text{III}}\text{Cl}_5^{2-}(\text{C}_{4\text{V}})\cdots\text{Cl}^\bullet]$. Intermediates like this (traditionally called radical pairs) are typical for Adamson redox mechanism of photosolvation of transition metal complexes [57]. Based on this interpretation, we propose that the SADS shown in Fig. 8 belong to the Franck–Condon excited state of $\text{Pt}^{\text{IV}}\text{Cl}_6^{2-}$ (curve 1), vibrationally hot (curve 2) and vibrationally cooled (curve 3) radical pair. The corresponding mechanism of primary processes is represented by Eqs. (32)–(36).



Generally, primary mechanism (Eqs. (32)–(36)) is the same as proposed in Ref. [26] for the case of methanol solutions. It contains an intermediate of Pt(III), namely $\text{Pt}^{\text{III}}\text{Cl}_6^{3-}$ complex, which is not observed in the available spectral range. The characteristic time of Reaction (36) is less than 50 ns, therefore, it is not observed in nanosecond laser flash photolysis experiments. The formation of the $\text{Pt}^{\text{III}}\text{Cl}_5^{2-}$ complex initiates the chain process of photosolvation described by Mechanism B.

5. Conclusions

In this work, the chain photosolvation of the $\text{Pt}^{\text{IV}}\text{Cl}_6^{2-}$ complex in acetonitrile is experimentally studied from the absorption of a light quantum to the formation of the final reaction products. In contrast to the previous work [37], it is shown that the primary photochemical process is the inter-sphere electron transfer from a solvent molecule to the light-excited complex. Experiments on ultrafast kinetic spectroscopy allowed us to construct the mechanism of electron transfer with the participation of the key intermediate interpreted as the primary Adamson radical pair $[\text{Pt}^{\text{III}}\text{Cl}_5^{2-}(\text{C}_{4\text{V}})\cdots\text{Cl}^\bullet]$. As we mentioned in [19], intermediates postulated for $\text{Pt}^{\text{IV}}\text{Cl}_6^{2-}$ photolysis should be verified against high-level quantum chemical calculations.

Acknowledgement

The financial support of the Russian Science Foundation (Grant 15-13-10012) is gratefully acknowledged.

References

- [1] L. Zang, W. Macyk, C. Lange, W.F. Mayer, C. Antonius, D. Meissner, H. Kish, Visible-light detoxification and charge generation by transition metal chloride modified titania, *Chem. Eur. J.* 6 (2000) 379–384.
- [2] W. Macyk, H. Kish, Photosensitization of crystalline and amorphous titanium dioxide by platinum(IV) chloride surface complexes, *Chem. Eur. J.* 7 (2001) 1862–1867.
- [3] X.Z. Li, F.B. Li, The enhancement of photodegradation efficiency using Pt–TiO₂ catalyst, *Chemosphere* 48 (2002) 1103–1111.
- [4] H. Kish, Chapter 9—visible light photocatalysis by metal halide complexes containing titania as a semiconductor ligand, *Adv. Inorg. Chem.* 63 (2011) 371–393.
- [5] F. Mahlamvana, R.J. Kriek, Photocatalytic reduction of platinum(II and IV) from their chloro complexes in a titanium dioxide suspension in the absence of an organic sacrificial reducing agent, *Appl. Catal. B: Environ.* 148–149 (2014) 387–393.
- [6] Q. Li, Zh. Chen, X. Zheng, Zh. Jin, Study of Photoreduction of PtCl_6^{2-} on CdS, *J. Phys. Chem.* 96 (1992) 5959–5962.
- [7] Zh. Jin, Zh. Chen, Q. Li, Ch. Xi, X. Zheng, On the conditions and mechanism of PtO_2 formation in the photoinduced conversion of H_2PtCl_6 , *J. Photochem. Photobiol. A: Chem.* 81 (1994) 177–182.
- [8] C. Harris, P.V. Kamat, Photocatalytic events of CdSe quantum dots in confined media. electrodic behavior of coupled platinum nanoparticles, *ACS Nano* 4 (2010) 7321–7330.
- [9] R.E. Cameron, A.B. Bocarsly, Photoactivated oxidation of alcohols by oxygen, *J. Am. Chem. Soc.* 107 (1985) 6116–6117.
- [10] R.E. Cameron, A.B. Bocarsly, Multielectron-photoinduced reduction of chloroplatinum complexes: visible light deposition of platinum metal, *Inorg. Chem.* 25 (1986) 2910–2913.
- [11] M. Sakamoto, M. Fujistuka, T. Majima, Light as a construction tool of metal nanoparticles: synthesis and mechanism, *J. Photochem. Photobiol. C: Photochem. Rev.* 10 (2009) 33–56.
- [12] N. Toshima, T. Takahashi, Colloidal dispersions of platinum and palladium clusters embedded in the micelles—preparation and application to the catalysis for hydrogenation of olefins, *Bull. Chem. Soc. Jpn.* 65 (1992) 400–409.
- [13] N. Toshima, K. Nakata, H. Kitoh, Giant platinum clusters with organic ligands: preparation and catalysis, *Inorg. Chim. Acta* 265 (1997) 149–153.
- [14] H. Einaga, M. Harada, Photochemical preparation of poly(*N*-vinyl-2-pyrrolidone)-stabilized platinum colloids and their deposition on titanium dioxide, *Langmuir* 21 (2005) 2578–2584.
- [15] M. Harada, K. Okamoto, M. Terazima, Diffusion of platinum ions and platinum nanoparticles during photoreduction processes using the transient grating method, *Langmuir* 22 (2006) 9142–9149.
- [16] M. Harada, H. Einaga, Formation mechanism of Pt particles by photoreduction of Pt ions in polymer solutions, *Langmuir* 22 (2006) 2371–2377.
- [17] Yu. Borodko, P. Ercius, D. Zhrebetsky, Y. Wang, Y. Sun, G. Somorjai, From single atoms to nanocrystals: photoreduction of $[\text{PtCl}_6]^{2-}$ in aqueous and tetrahydrofuran solutions of PVP, *J. Phys. Chem. C* 117 (2013) 26667–26674.
- [18] H. Chang, Y. Tsai, C. Cheng, C. Lin, P. Wu, Preparation of graphene-supported platinum nanoparticles in aqueous solution by femtosecond laser pulses for methanol oxidation, *J. Power Sources* 239 (2013) 164–168.
- [19] E.M. Glebov, I.P. Pozdnyakov, V.F. Plyusnin, I. Khmelinskii, Primary reactions in photochemistry of hexahalide complexes of platinum group metals: a minireview, *J. Photochem. Photobiol. C: Photochem. Rev.* 24 (2015) 1–15.
- [20] L.E. Cox, D.G. Peters, E.L. Wehry, Photoaquation of hexachloroplatinate(IV), *J. Inorg. Nucl. Chem.* 14 (1972) 297–305.
- [21] R.C. Wright, G.S. Laurence, Production of platinum(III) by flash photolysis of PtCl_6^{2-} , *J. Chem. Soc. Chem. Commun.* (1972) 132–133.
- [22] K.P. Balashev, V.V. Vasil'ev, M. A. Zimnyakov, G. A. Shagisultanova, Kinetics of chain reactions of photoaquation involving platinum(III) complexes, *Koord. Khim.* 984 (2016) 976–980 (in Russian).
- [23] K.P. Balashev, I.I. Blinov, G.A. Shagisultanova, Acidic-basic properties of platinum(III) chloride complexes, *Zh. Neorg. Khim.* 32 (1987) 2470–2474 (in Russian).
- [24] W.L. Waltz, J. Lillie, A. Goursot, H. Chermette, Photolytic and radiolytic study of platinum(III) complex ions containing aquo and chloro ligands, *Inorg. Chem.* 28 (1989) 2247–2256.
- [25] I.V. Znakovskaya, Yu.A. Sosodova, E.M. Glebov, V.P. Grivin, V.F. Plyusnin, Intermediates formed by laser flash photolysis of PtCl_6^{2-} complex in aqueous solutions, *Photochem. Photobiol. Sci.* 4 (2005) 897–902.
- [26] E.M. Glebov, A.V. Kolomeets, I.P. Pozdnyakov, V.F. Plyusnin, V.P. Grivin, N.V. Tkachenko, H. Lemmetyinen, Redox processes in photochemistry of Pt(IV) hexahaloid complexes, *RSC Adv.* 2 (2012) 5768–5778.
- [27] E.M. Glebov, A.V. Kolomeets, I.P. Pozdnyakov, V.P. Grivin, V.F. Plyusnin, N.V. Tkachenko, H. Lemmetyinen, Chain processes in the photochemistry of Pt(IV) halide complexes in aqueous solutions, *Russ. Chem. Bull.* 62 (2013) 1540–1548.
- [28] R.L. Rich, H. Taube, Catalysis by Pt(III) of exchange reactions of PtCl_4^{2-} and PtCl_6^{2-} , *J. Am. Chem. Soc.* 76 (1954) 2608–2611.
- [29] A. Goursot, A.D. Kirk, W.L. Waltz, G.B. Porter, D.K. Sharma, Experimental and theoretical study of the nascent photoredox behavior of the aqueous hexachloroplatinate(IV) ion, *Inorg. Chem.* 26 (1987) 14–18.
- [30] I.P. Pozdnyakov, E.M. Glebov, S.G. Matveeva, V.F. Plyusnin, A.A. Melnikov, S.V. Chekalin, Ultrafast photophysical and photochemical processes caused by UV-

- excitation of PtBr_6^{2-} and PtCl_6^{2-} complexes in water and methanol, Russ. Chem. Bull. 8 (2015) 1784–1795 (in Russian).
- [31] V.P. Grivin, I.V. Khmelinski, V.F. Plyusnin, I.I. Blinov, K.P. Balashev, Photochemistry of PtCl_6^{2-} complex in methanol solution, J. Photochem. Photobiol. A: Chem. 51 (1990) 167–178.
- [32] V.P. Grivin, I.V. Khmelinski, V.F. Plyusnin, Intermediates in the photoreduction of PtCl_6^{2-} in methanol, J. Photochem. Photobiol. A: Chem. 51 (1990) 379–389.
- [33] V.P. Grivin, I.V. Khmelinski, V.F. Plyusnin, Primary photochemical processes of the PtCl_6^{2-} complex in alcohols, J. Photochem. Photobiol. A: Chem. 59 (1991) 153–161.
- [34] M. Wojnicki, P. Kwolek, Reduction of hexachloroplatinate(IV) ions with methanol under UV radiation, J. Photochem. Photobiol. A: Chem. 314 (2016) 133–142.
- [35] O. Monreal, T. Esmaeli, P.E. Hoggard, A kinetic study of the photoreduction of hexachloroplatinate(IV) in chloroform, Inorg. Chim. Acta 265 (1997) 279–282.
- [36] P.E. Hoggard, A. Vogler, The photooxidation of tetrachloroplatinate(II) in chloroform, Inorg. Chim. Acta 348 (2003) 229–232.
- [37] K.P. Balashev, I.I. Blinov, G.A. Shagisultanova, Kinetics and mechanism for photosubstitution of the $[\text{PtCl}_6^{2-}]$ ion in acetonitrile, Kinet. Catal. 28 (1987) 696–700.
- [38] A. Goursot, H. Chermette, E. Peigault, M. Chanon, W.L. Waltz, X α method as a tool for structure elucidation of short-lived transients generated by pulse radiolysis or flash photolysis. II. Oxidative reactions of PtCl_4^{2-} , Inorg. Chem. 24 (1985) 1042–1047.
- [39] D.J. Adams, S. Barlow, G.V. Buxton, T.M. Malone, G.A. Salmon, Evaluation of the stability constants of Cl_2^- in neutral aqueous solutions, J. Chem. Soc. Faraday Trans. 91 (1995) 3303–3305.
- [40] E. Sosnin, T. Oppenlander, V. Tarasenko, Applications of capacitive and barrier discharge excilamps in photoscience, J. Photochem. Photobiol. C: Photochem. Rev. 7 (2006) 145–163.
- [41] I.P. Pozdnyakov, V.F. Plyusnin, V.P. Grivin, D.Yu. Vorobyev, N.M. Bazhin, S. Pages, E. Vauthey, J. Photochem. Photobiol. A: Chem. 181 (2006) 37–43.
- [42] S.V. Chekalin, The unique femtosecond spectroscopic complex as an instrument for ultrafast spectroscopy: femtochemistry and nanooptics, Phys. Usp. 49 (2006) 634–641.
- [43] D.L. Swihart, W.R. Mason, Electronic spectra of octahedral platinum(IV) complexes, Inorg. Chem. 9 (1970) 1749–1757.
- [44] A. Goursot, E. Penigault, H. Chermette, Relativistic MS X α calculations of the electronic structure and related properties of PtCl_6^{2-} , Chem. Phys. Lett. 97 (1983) 215–220.
- [45] A. Goursot, H. Chermette, E. Penigault, M. Chanon, W.L. Waltz, X α method as a tool for structure elucidation of short-lived transients generated by pulse radiolysis or flash photolysis. I. Reductive reactions of PtCl_6^{2-} , Inorg. Chem. 23 (1984) 3618–3625.
- [46] U. Lachish, A. Shaffer, G. Stein, Intensity dependence in laser flash photolysis experiments: hydrated electron formation from ferrocyanide tyrosine, and tryptophan, J. Chem. Phys. 64 (1976) 4205–4211.
- [47] V.B. Kogan, Spravochnik po rastvorimosti (Solubility Handbook), Vol. 1, Book 1, Moscow, 1970, P. 739 (in Russian).
- [48] X.-Y. Yu, Critical evaluation of rate constants and equilibrium constants of hydrogen peroxide photolysis in aqueous acidic solutions containing chloride ions, J. Phys. Chem. Ref. Data 33 (2004) 747–764.
- [49] D.J. Adams, S. Barlow, G.V. Buxton, T.M. Malone, G.A. Salmon, Evaluation of the stability constants of Cl_2^- in neutral aqueous solutions, J. Chem. Soc. Faraday Trans. 91 (1995) 3303–3305.
- [50] J. Richardi, P.H. Fries, H. Krienke, The solvation of ions in acetonitrile and acetone: a molecular Ornstein–Zernike study, J. Chem. Phys. 108 (1998) 4079–4089.
- [51] E.P. Grimpsrud, B. Kratochvil, Second-order rate constants and ion association in aprotic solvents by high-pressure conductance, J. Am. Chem. Soc. 95 (1973) 4477–4483.
- [52] I.G. Draganic, Z.D. Draganic, V.M. Markovic, The pulse radiolysis of aqueous solutions of simple RCN compounds, Int. J. Radiat. Phys. Chem. 8 (1976) 339–342.
- [53] S. Mosseri, P. Neta, P. Meisel, The mechanism of cyanide release in the radiolysis of acetonitrile. formation and decay of the cyanomethylperoxy radical, Radiat. Phys. Chem. 36 (1990) 683–687.
- [54] J.Q. Wu, I. Beranek, H. Fischer, Absolute rate constants for the addition of the cyanomethyl (CH_2CN) and (tert-butoxy)carbonylmethyl ($\text{CH}_2\text{CO}_2\text{C}(\text{CH}_3)_3$) radicals to alkenes in solutions, Helv. Chim. Acta 78 (1995) 194–214.
- [55] L. Palfrey, T.F. Heinz, Coherent interactions in pump-probe absorption measurements: the effect of phase gratings, J. Opt. Soc. Am. B 2 (1985) 674–679.
- [56] A.S. Rury, R.J. Sension, Broadband ultrafast transient absorption of iron(III) tetraphenylporphyrin chloride in the condensed phase, Chem. Phys. 422 (2013) 220–228.
- [57] A.W. Adamson, A.H. Sporer, Photochemistry of complex ions. I. Some photochemical reactions of aqueous PtBr_6^{2-} , $\text{Mo}(\text{CN})_8^{4-}$, and various Co(III) and Cr(III) complex ions, J. Am. Chem. Soc. 80 (1958) 3865–3870.